

Electronic Supplementary Information

A Three-Dimensional Lead Iodide Perovskite Analog Featuring Hydrogen-bonded Dual Monovalent Cations

Wei Wang, Cheng-Dong Liu, Chang-Chun Fan, Wen Zhang*

Jiangsu Key Laboratory for Science and Applications of Molecular Ferroelectrics and School of Chemistry and Chemical Engineering, Southeast University, Nanjing 211189, China.

Email: zhangwen@seu.edu.cn

Experimental section

Starting materials

Morpholine (98%), ammonium iodide (98%), lead iodide (PbI₂, 99.9%), and hydroiodic acid (HI, 57 wt.% in H₂O) were commercially available and used as received without further purification.

Synthesis of 1. PbI₂ powder (2 mmol, 0.922 g) and morpholine (2 mmol, 0.174 g) were dissolved in a solution containing 5 mL of aqueous HI and 0.1 mL of H₃PO₂. The mixture was heated above 110°C, then NH₄I (4 mmol, 0.579 g) was added. The solution was gradually cooled to 90°C, during which red crystals or powder of compound **1** began to precipitate at the bottom of the beaker. The solution was left for additional hours to promote further crystal growth. Alternatively, compound **1** can also be synthesized at room temperature; however, this requires more NH₄I and often results in a mixture of the desired phase and a morpholinium-based phase. Anal. Calcd. for C₄H₁₄N₂OPb₂I₆ (**1**): C, 3.75%; H, 1.10%; N, 2.19%; O, 1.25%. Found: C: 3.99%, H: 1.22%, N: 2.17%; O, 1.17%.

General characterizations. PXRD patterns were collected using a Rigaku SmartLab X-ray diffraction system. Thermogravimetric analysis (TGA) was performed using a NETZSCH TG209 F3 instrument for TGA, with a heating rate of 10 °C min⁻¹ under a nitrogen atmosphere. Ultraviolet-visible (UV-Vis) diffuse reflection spectra were acquired using a Shimadzu UV2600 spectrophotometer equipped with an ISR-2600Plus integrating sphere. Low frequency Raman spectra were acquired using 633 nm laser excitation on a HORIBA LabRAM HR Evolution equipment. The spectra were collected from -300 cm⁻¹ to 300 cm⁻¹. The FT-IR spectra were recorded using Nicolet iS50 instrument with a transmission method. The sample of **1** was mixed with KBr and prepared as a KBr pellet (1% *wt*). Photoluminescence (PL) spectra were obtained through analysis on an Edinburgh FLS1000 steady-state/transient-state fluorescence spectrometer. Elemental analysis was performed using the Elementar Vario Micro Cube. The CHN determination method involves combusting the sample while the O method employs high-temperature cracking.

Single-crystal X-ray Diffraction. Crystallographic data of the compound were collected on a Rigaku Oxford Diffraction Supernova Dual Source, Cu at Zero equipped with an AtlasS2 CCD using Mo K α radiation and an XtaLAB Synergy R, DW system, HyPix diffractometer. CrystalClear 1.3.5 package was used to collect data, refine cells, and reduce data. SHELXL-2014 package was used to solve the structures by direct methods. All non-hydrogen atoms were

refined anisotropically. All the hydrogen atoms were generated geometrically. CCDC 2387432 contain the crystallographic data.

I-V Measurement. A 565 nm LED (M565L3-M0087 1936, Thorlabs) was used. The light beam was concentrated between two electrodes fabricated from a silver coating on the crystal. Current signals were gathered by using a PDA FS-Pro 380 current meter. Light intensity was assessed by using a Si photodetector linked to a power meter (PM120VA, Thorlabs).

Theoretical calculations. DFT calculations were performed by using the Vienna ab initio simulation package.¹ The input structures were built by using the crystallographic data and optimized by fixing the cell. Thresholds of convergence criteria are set as 10^{-7} eV and 0.02 eV/Å for energy differences during electronic steps and maximum forces in geometry optimization. The Perdew–Burke–Ernzerhof (PBE) functional within the generalized gradient approximation (GGA) was adopted to express exchange-correlation interaction.^{2,3} The van der Waals interactions were evaluated by adopting DFT-D3 method.⁴ The ion–electron interactions were described by projector augmented wave (PAW) potentials with the energy cutoff of 500 eV. The VASPKIT was used to perform postprocessing analysis.⁵

References

- (1) Kresse, G.; Furthmüller, J. Efficient Iterative Schemes for Ab Initio Total-Energy Calculations Using a Plane-Wave Basis Set. *Phys. Rev. B* **1996**, *54*, 11169-11186.
- (2) Blöchl, P. E. Projector Augmented-Wave Method. *Phys. Rev. B* **1994**, *50*, 17953-17979.
- (3) Perdew, J. P.; Burke, K.; Ernzerhof, M. Generalized Gradient Approximation Made Simple. *Phys. Rev. Lett.* **1996**, *77*, 3865-3868.
- (4) Grimme, S.; Antony, J.; Ehrlich, S.; Krieg, H. A Consistent and Accurate Ab Initio Parametrization of Density Functional Dispersion Correction (DFT-D) for the 94 Elements H-Pu. *J. Chem. Phys.* **2010**, *132*, 154104.
- (5) Wang, V.; Xu, N.; Liu, J.-C.; Tang, G.; Geng, W.-T. Vaspkit: A User-Friendly Interface Facilitating High-Throughput Computing and Analysis Using Vasp Code. *Comput. Phys. Commun.* **2021**, *267*, 108033.

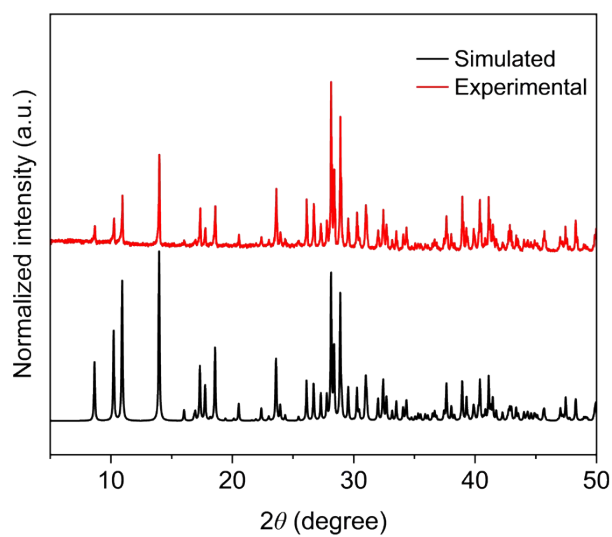


Fig. S1 PXRD pattern of **1**.

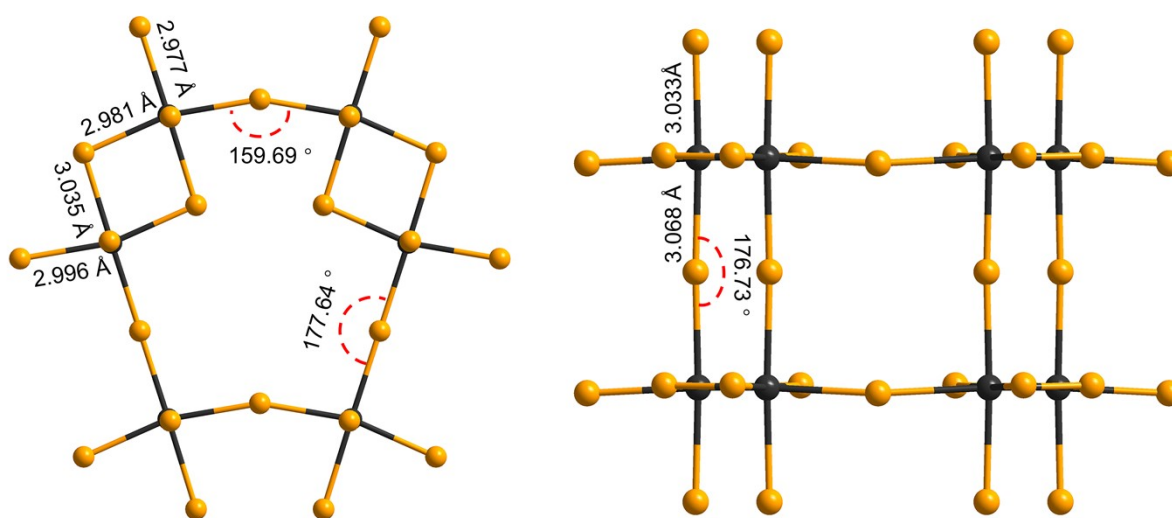


Fig. S2 Summary of bond angles of $(\text{TMEA})\text{Pb}_2\text{Br}_6$ between inter-dimer Pb–I–Pb bonds and bond lengths within each octahedron.

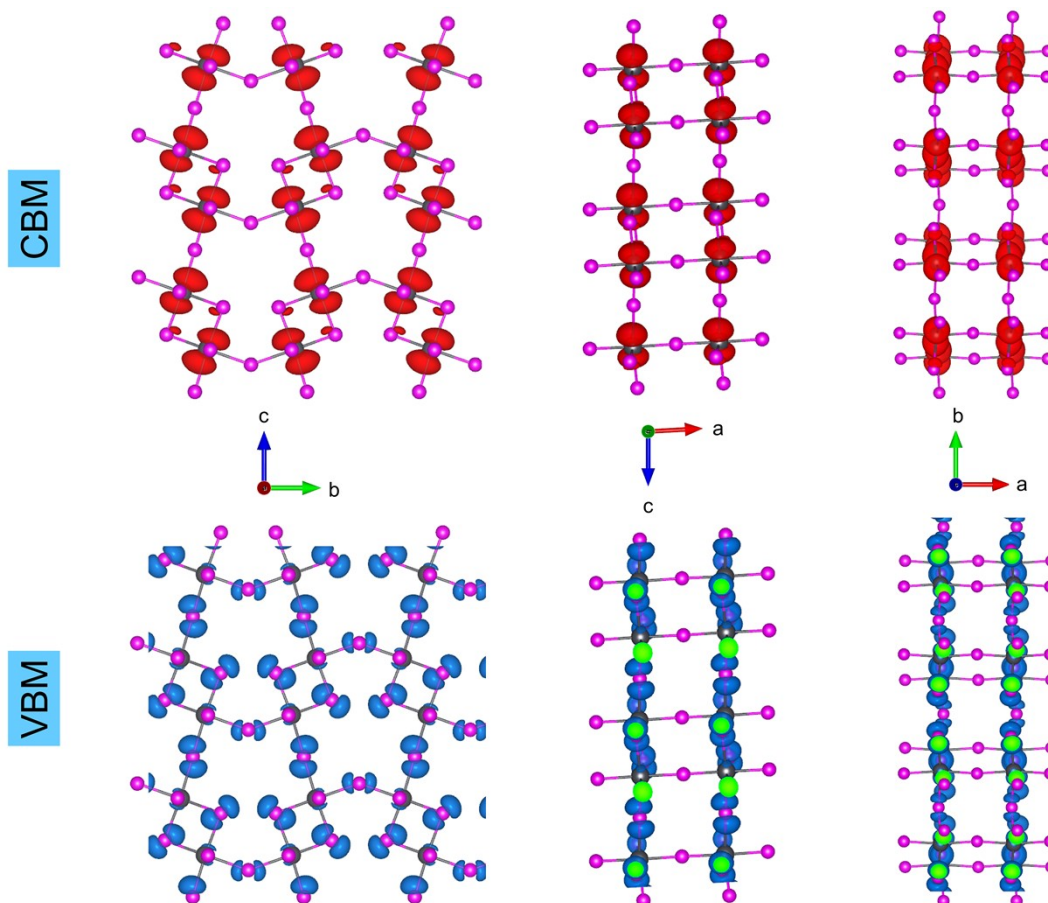


Fig. S3 Partial charge densities of the CBM and the VBM observed from different direction.

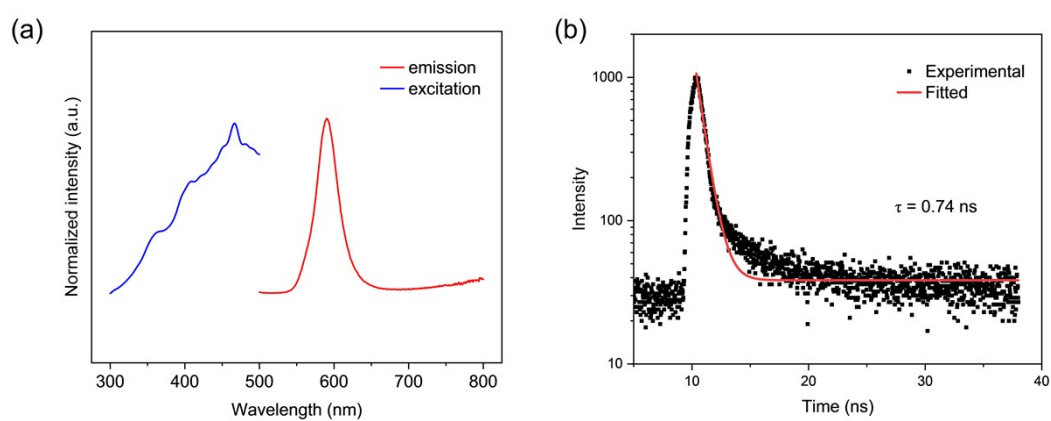


Fig. S4 (a) Photoluminescence excitation and emission spectrum of **1**.(b) PL decay curve of **1** monitoring at 590 nm.

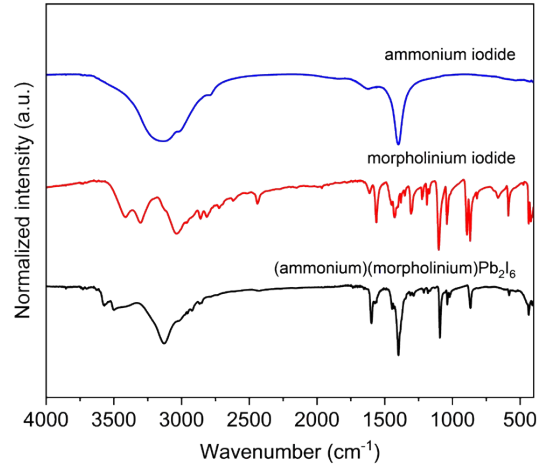


Fig. S5 Fourier transform infrared spectroscopy of **1**.

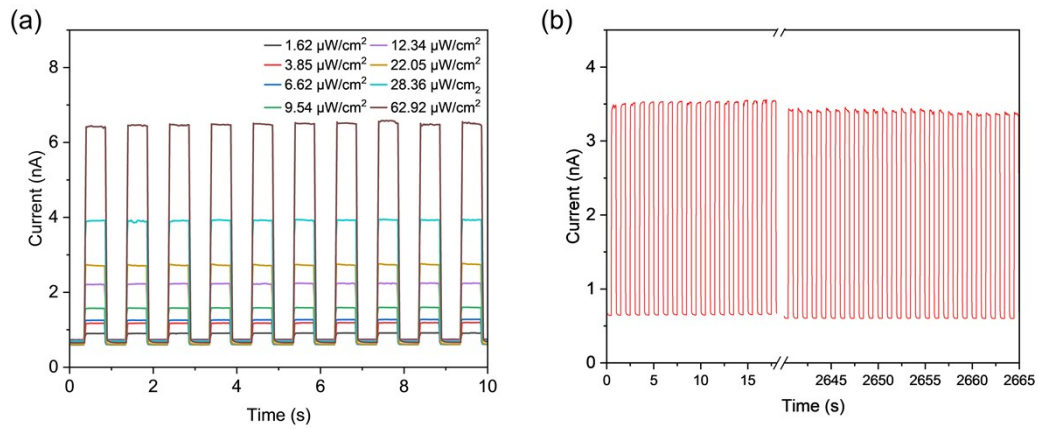


Fig. S6 On-off switching under varying light powers with a 1 V bias. (b) time-dependent switching cycles of photocurrent response at 565 nm.

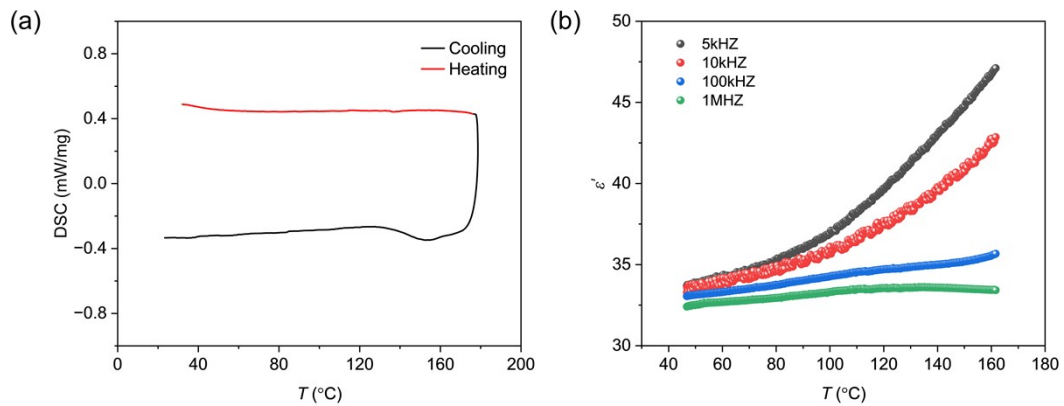


Fig. S7 DSC (a) and Dielectric (b) measurements of **1**.

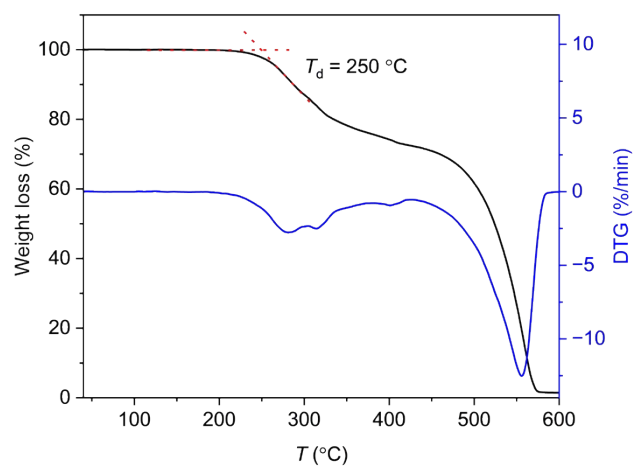


Fig. S8 TGA curve of **1**.

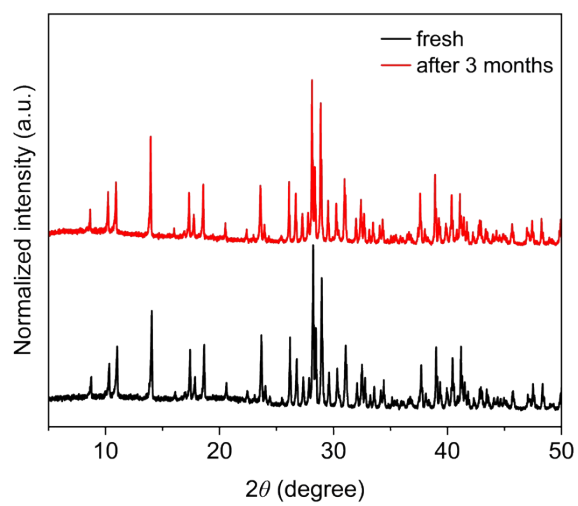


Fig. S9 PXRD patterns of fresh sample and the one after 3 months.

Table S1. Crystallographic data and refinement parameters of **1**.

| | 1 |
|---|---|
| <i>T</i> / K | 152.98(10) K |
| Formula | (NH ₄)(C ₄ H ₁₀ NO)Pb ₂ I ₆ |
| Formula weight | 1281.95 |
| Crystal system | monoclinic |
| Space group | <i>P</i> 2 ₁ / <i>m</i> |
| <i>a</i> / Å | 6.3366(3) |
| <i>b</i> / Å | 16.1613(7) |
| <i>c</i> / Å | 10.1821(4) |
| <i>α</i> / ° | 90 |
| <i>β</i> / ° | 93.579(4) |
| <i>γ</i> / ° | 90 |
| Volume / Å ³ | 1040.69(8) |
| <i>Z</i> | 2 |
| <i>D</i> _{calc} / g·cm ⁻³ | 4.091 |
| <i>μ</i> / mm ⁻¹ | 25.042 |
| <i>F</i> (000) | 1084.0 |
| 2 <i>θ</i> range / ° | 4.008–61.856 |
| Reflns collected | 7163 |
| Independent reflns (<i>R</i> _{int}) | 2731(0.0333) |
| no. parameters | 86 |
| GOF | 1.013 |
| <i>R</i> ₁ ^[a] , <i>wR</i> ₂ ^[b] [<i>I</i> ≥ 2σ(<i>I</i>)] | 0.0347, 0.0987 |
| <i>R</i> ₁ , <i>wR</i> ₂ [all data] | 0.0381, 0.1003 |
| Δρ ^[c] / e·Å ⁻³ | 2.24, -2.36 |

^[a] $R_1 = \sum ||F_o| - |F_c|| / \sum |F_o|$.

^[b] $wR_2 = [\sum w(F_o^2 - F_c^2)^2 / \sum w(F_o^2)^2]^{1/2}$.

^[c] Maximum and minimum residual electron density.

Table S2. Summary of hydrogen bonds.

| Hydrogen bonds for 1 | | | | |
|--|---------|-----------|-----------|----------|
| D–H···A | D–H / Å | H···A / Å | D···A / Å | ∠DHA / ° |
| N(1)–H(1C)···I(2) ⁱ | 0.89(3) | 2.86(3) | 3.628(7) | 145(4) |
| N(1)–H(1E)···O(1) | 0.89(3) | 1.86(3) | 2.732(15) | 165(11) |
| N(2)–H(2A)···I1(1) | 0.91 | 2.75 | 3.658(11) | 176 |
| N(2)–H(2B)···I(1) ⁱⁱ | 0.91 | 2.72 | 3.610(11) | 166 |
| Symmetry codes: (i) $x, 3/2-y, 1+z$; (ii) $1+x, y, z$ | | | | |

Table S3. Bond angles and bond lengths of **1**.

| Bond angles | Angle / ° | Bond lengths | Length / Å |
|---|--------------|--------------------------|------------|
| I(2)—Pb(1)—I(1) | 85.879 (18) | Pb(1)—I(1) | 3.3065 (4) |
| I(2) ⁱ —Pb(1)—I(1) | 87.787 (18) | Pb(1)—I(2) | 3.1600 (5) |
| I(2)—Pb(1)—I(2) ⁱ | 173.60 (3) | Pb(1)—I(2) ⁱ | 3.1865 (5) |
| I(2)—Pb(1)—I(3) ⁱⁱ | 89.329 (16) | Pb(1)—I(3) ⁱⁱ | 3.2331 (6) |
| I(2) ⁱ —Pb(1)—I(3) ⁱⁱ | 89.298 (15) | Pb(1)—I(3) | 3.1157 (6) |
| I(2)—Pb(1)—I(4) | 94.440 (13) | Pb(1)—I(4) | 3.1703 (3) |
| I(3) ⁱⁱ —Pb(1)—I(1) | 85.755 (17) | | |
| I(3)—Pb(1)—I(1) | 174.506 (18) | | |
| I(3)—Pb(1)—I(2) ⁱ | 96.629 (17) | | |
| I(3)—Pb(1)—I(2) | 89.643 (17) | | |
| I(3)—Pb(1)—I(3) ⁱⁱ | 91.017 (15) | | |
| I(3)—Pb(1)—I(4) | 94.252 (12) | | |
| I(4)—Pb(1)—I(1) | 89.273 (15) | | |
| I(4)—Pb(1)—I(2) ⁱ | 86.379 (12) | | |
| I(4)—Pb(1)—I(3) ⁱⁱ | 173.535 (13) | | |
| Pb(1)—I(1)—Pb(1) ⁱⁱⁱ | 146.16 (3) | | |
| Pb(1)—I(2)—Pb(1) ^{iv} | 173.60 (3) | | |
| Pb(1)—I(3)—Pb(1) ⁱⁱ | 88.982 (15) | | |
| Pb(1) ^v —I(4)—Pb(1) | 180.0 | | |

Symmetry codes: (i) $x-1, y, z$; (ii) $-x-1, -y+1, -z$; (iii) $x, -y+3/2, z$; (iv) $x+1, y, z$; (v) $-x-1, -y+1, -z+1$.

Table S4. Calculated volume of some cations.

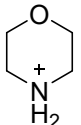
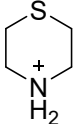
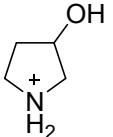
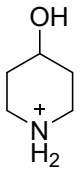
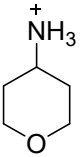
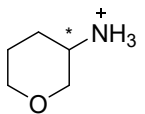
| | Cations | Volume (Å ³) | Volume difference | Reference for used CIFs |
|---|---|--------------------------|-------------------|-------------------------------|
| 1 |  morpholinium | 157 | 0 | This work |
| 2 |  thiomorpholinium | 150 | -4.5% | 10.1016/j.ccllet.2021.07.039 |
| 3 |  3-hydroxypyrrolidin-1-ium | 128 | -18.5% | 10.1063/5.0035793 |
| 4 |  4-hydroxypiperidinium | 153 | 2.5% | 10.1107/S010827019900956 7 |
| 5 |  tetrahydro-2H-pyran-4-aminium | 153 | 2.5% | 10.1021/jacs.9b12368 |
| 6 |  (dihydro-2H-3λ ³ -pyran-3(4H)-yl)ammonium | 176 | 12.1% | 10.1039/d4tc01531b |

Table S5. Calculated hole (m_h) and electron (m_e) effective mass for **1**.

| direction | effective mass(m_0) | |
|-----------|-------------------------|-------|
| | m_h | m_e |
| <i>a</i> | -0.290 | 0.085 |
| <i>b</i> | -0.568 | 3.503 |
| <i>c</i> | -0.481 | 1.519 |